AMERICAN SOCIETY FOR MICROBIOLOGY | Applied and Environmental Microbiology®

INVERTEBRATE MICROBIOLOGY

Essential Roles of Two FRQ Proteins (Frq1 and Frq2) in *Beauveria bassiana*'s Virulence, Infection Cycle, and Calcofluor-Specific Signaling

Sen-Miao Tong,[a] Ben-Jie Gao,[b] Han Peng,[b] Ming-Guang Feng[b]

[a]College of Agricultural and Food Science, Zhejiang A & F University, Lin'an, Zhejiang, China

[b]MOE Laboratory of Biosystems Homeostasis & Protection, Institute of Microbiology, Institute of Microbiology, College of Life Sciences, Zhejiang University, Hangzhou, Zhejiang, China

ABSTRACT Two FRQ proteins (Frq1 and Frq2) distinct in molecular mass and structure coexist in *Beauveria bassiana*, an asexual insect-pathogenic fungus. Frq1 and Frq2 have been proven to have opposite nuclear rhythms that can persistently activate developmental activator genes and hence orchestrate nonrhythmic conidiation *in vitro* under light or in darkness. Here, we report the essentiality of either FRQ, but Frq2 being more important than Frq1, for the fungal virulence and infection cycle. The fungal virulence was attenuated significantly more in the absence of *frq2* than in the absence of *frq1* through either normal cuticle infection or cuticle-bypassing infection by intrahemocoel injection, accompanied by differentially reduced secretion of Pr1 proteases required for the cuticle infection and delayed development of hyphal bodies *in vivo*, which usually propagate by yeast-like budding in the host hemocoel to accelerate insect death from mycosis. Despite insignificant changes in radial growth under normal, oxidative, and hyperosmotic culture conditions, conidial yields of the Δ*frq1* and Δ*frq2* mutants on insect cadavers were sharply reduced, and the reduction increased with shortening daylight length on day 9 or 12 after death, indicating that both Frq1 and Frq2 are required for the fungal infection cycle in host habitats. Intriguingly, the Δ*frq1* and Δ*frq2* mutants showed hypersensitivity and high resistance to cell wall-perturbing calcofluor white, coinciding respectively with the calcofluor-triggered cells' hypo- and hyperphosphorylated signals of Slt2, a mitogen-activated protein kinase (MAPK) required for mediation of cell wall integrity. This finding offers a novel insight into opposite roles of Frq1 and Frq2 in calcofluor-specific signal transduction via the fungal Slt2 cascade.

IMPORTANCE Opposite nuclear rhythms of two distinct FRQ proteins (Frq1 and Frq2) coexisting in an asexual fungal insect pathogen have been shown to orchestrate the fungal nonrhythmic conidiation *in vitro* in a circadian day independent of photoperiod change. This paper reports essential roles of both Frq1 and Frq2, but a greater role for Frq2, in sustaining the fungal virulence and infection cycle since either *frq1* or *frq2* deletion led to marked delay of lethal action against a model insect and drastic reduction of conidial yield on insect cadavers. Moreover, the *frq1* and *frq2* mutants display hypersensitivity and high resistance to cell wall perturbation and have hypo- and hyperphosphorylated MAPK/Slt2 in calcofluor white-triggered cells, respectively. These findings uncover a requirement of Frq1 and Frq2 for the fungal infection cycle in host habitats and provide a novel insight into their opposite roles in calcofluor-specific signal transduction through the MAPK/Slt2 cascade.

KEYWORDS entomopathogenic fungi, frequency proteins, gene mutagenesis, pathogenicity, asexual cycle, cell wall integrity, biological control

Citation Tong S-M, Gao B-J, Peng H, Feng M-G. 2021. Essential roles of two FRQ proteins (Frq1 and Frq2) in *Beauveria bassiana*'s virulence, infection cycle, and calcofluor-specific signaling. Appl Environ Microbiol 87:e02545-20. https://doi.org/10.1128/AEM.02545-20.

Editor Irina S. Druzhinina, Nanjing Agricultural University

Address correspondence to Sen-Miao Tong, tongsm@zafu.edu.cn, or Ming-Guang Feng, mgfeng@zju.edu.cn.

Received 15 October 2020
Accepted 11 December 2020
Accepted manuscript posted online 4 January 2021
Published 26 February 2021

Filamentous fungal pathogens that undergo the asexual cycle alone rely upon a capability of aerial conidiation for survival and dispersal in host habitats. The process of conidiation is genetically regulated by the central developmental pathway (CDP) that is activated by signal transducers in the upstream development activation (UDA) pathway such as FluG and FlbA to FlbE (1). The UDA pathway has three FluG-cored routes (FluG/FlbA, FluG/FlbE/FlbB/FlbD, and FluG/FlbC) to activate the key CDP activator gene *brlA*, which enables sequential activation of *abaA* and *wetA*, two other CDP genes required for conidiation and conidial maturation in some model fungi (reviewed in references 2, 3).

The three CDP activator genes have been shown to control the aerial conidiation process in the insect-pathogenic fungus *Beauveria bassiana* as they do in the model fungi because the fungal conidiation was completely abolished in the absence of *brlA* or *abaA* (4) and nearly abolished in the absence of *wetA* (5). Previous studies have revealed that the CDP activation can be achieved through multiple routes other than the UDA pathway in *B. bassiana*. In the studies, severe or extremely severe defects in aerial conidiation concurred with sharply reduced transcript levels of *brlA*, *abaA*, and *wetA* in single disruption mutants of many genes involved in various pathways. As examples in *B. bassiana*, these genes encode the Na^+/H^+ antiporter Nhx1 (6), the vacuolar protein VLP4 (7), the blue light receptor VVD (8), the histone acetyltransferases Gcn5 and Mst2 (9, 10), the histone deacetylases Rpd3 and Hos2 (11, 12), the components of mitogen-activated protein kinase (MAPK) Fus3 cascade (13, 14), the two frequency (FRQ) proteins Frq1 and Frq2 (15), the DNA damage repair protein Rad23 (16), and the polyubiquitin precursor Ubi4 (17). Particularly, the key CDP gene *brlA* can be activated through Gcn5-catalyzed histone H3K14 phosphorylation at critical sites of the gene promoter region (9). Opposite nuclear rhythms of Frq1 and Frq2 required for persistent activation of the three CDP genes in a circadian day have been shown to orchestrate nonrhythmic conidiation that speeds up with increasing daylight length and results in a maximal yield of $\sim 5.5 \times 10^8$ conidia/cm^2 plate culture within 7 to 9 days regardless of photoperiod change (15). Aside from the CDP-related genes, many others not involved in the CDP or the UDA pathway are also required for the fungal conidiation, such as the MAPK Ssk2 in the MAPK Hog1 cascade serving as a high-osmolarity glycerol (HOG) pathway (14) and the coding gene of Ssr4, a cosubunit of chromatin-remodeling SWI/SNF and RSC complexes required for global gene activity (18).

Among those required for conidiation of *B. bassiana*, Frq1 and Frq2 are of special interest due to a tight link of *in vitro* nonrhythmic conidiation to their daily opposite nuclear rhythms under the control of a unique FRQ-interacting RNA helicase (FRH), the inactivation of which repressed the *frq1* or *frq2* expression to a nearly undetectable level and abolished accumulation of Frq1 and Frq2 in both nucleus and cytoplasm (15). The nonrhythmic conidiation favors large-scale production of *B. bassiana* conidia as active ingredients of wide-spectrum fungal insecticides (19). This conidiation mode is distinguished from the rhythmic carotenoid-pigmented conidiospore production of *Neurospora crassa* under the control of a circadian clock, in which a unique FRQ protein forms the long and short isoforms l-FRQ and s-FRQ via thermosensitive splicing of the same gene at different codons (20–22) and serves as an oscillator, i.e., a core player in a transcription-translation feedback loop required for precise timing of the clock (reviewed in references 23, 24). Some fungi have diverse circadian clock proteins, such as *Fusarium oxysporum* vectoring up to 10 single FRQ domain-containing proteins (25), although functions of multiple clock proteins in a filamentous fungus have not yet been well explored. In *B. bassiana*, Frq1 (964 amino acids [aa]) features a single large FRQ domain (residues 13 to 953) similar to that of l-FRQ (989 aa) or s-FRQ (890 aa) in *N. crassa* and is structurally different from Frq2 (583 aa), which is much smaller in molecular size and has two short FRQ domains (residues 27 to 248 and 256 to 557) that are bridged by a 23-aa nuclear localization signal (NLS) motif (15). Both the structural differences and the opposite nuclear rhythms essential for the nonrhythmic conidiation demonstrate that Frq1 and Frq2 are not isoforms of the same gene as l-FRQ and s-FRQ

seen in *N. crassa* and also imply that the circadian system comprising two phase-complementary oscillators in *B. bassiana* could be much more complicated than, and hence very different from, the model system well characterized in *N. crassa* (reviewed in references 23 and 24).

As a wide-spectrum insect pathogen, *B. bassiana* is also a saprophytic fungus that exists in host habitats worldwide and has no real teleomorph ever found in nature or induced under laboratory conditions (26). The essential roles of both Frq1 and Frq2 in the nonrhythmic conidiation independent of photoperiod change suggest an importance of each in the fungal infection cycle (i.e., asexual cycle *in vivo*). No matter how Frq1 and Frq2 function in the complicated circadian system, this study seeks to elucidate their roles in the fungal infection cycle and virulence-related cellular events postinfection. As present below, both Frq1 and Frq2 are essential for the virulence and infection cycle of *B. bassiana*. Unexpectedly, we found opposite roles of Frq1 and Frq2 in calcofluor-specific signal transduction through the MAPK Slt2 cascade, which acts as the cell wall integrity (CWI) pathway required for fortification of the cell wall and resistance to cell wall perturbation in filamentous fungi (reviewed in reference 27) and insect mycopathogens (28; reviewed in reference 29).

RESULTS

Frq1 and Frq2 are essential for virulence and virulence-related cellular events. The deletion and complementation mutants of *frq1* and *frq2* created in the previous study (15) were assayed in parallel with the parental wild-type strain (designated WT herein) for their virulence to the fifth-instar larvae of the greater wax moth *Galleria mellonella* in two infection modes. Either topical application (immersion) of a 10^7 conidia/ml suspension for normal cuticle infection or intrahemocoel injection of ~500 conidia (5 μl of a 10^5 conidia/ml suspension) per larva for cuticle-bypassing infection resulted in marked differences of time-survival trends between two Δ*frq* mutants and three control (WT and complemented) strains (Fig. 1A). The mean (±SD) estimates of median lethal time (LT_{50}) made from probit analysis of the resultant time-mortality trends were 5.2 (±0.14) and 4.0 (±0.08) days for the WT strain against the larvae infected via the normal and cuticle-bypassing routes, respectively (Fig. 1B). In contrast, the LT_{50} estimates for the Δ*frq1* and Δ*frq2* mutants against the model insect increased to 9.6 (±0.52) and 12.6 (±0.15) days in the normal infection and 8.6 (±0.13) and 11.3 (±0.35) days in the cuticle-bypassing infection, respectively. These bioassay data demonstrated that the fungal lethal actions against the larvae through the two infection modes were prolonged, respectively, by 0.85- and 1.15-fold in the absence of *frq1* and by 1.44- and 1.82-fold in the absence of *frq2*. The largely attenuated virulence in either deletion mutant was well restored by targeted gene complementation. The results highlight an essentiality of either FRQ, but greater importance of Frq2 than of Frq1, for the virulence of *B. bassiana*.

The virulence of a fungal insect pathogen depends on not only the success of hyphal invasion into insect body by means of the activities of extracellular enzymes required for cuticle degradation (30), such as subtilisin-like Pr1 proteases collectively crucial for insect pathogenicity of *B. bassiana* (31), but also a speed of fungal intrahemocoel proliferation by yeast-like budding until host death as a result of mycosis development. The yeast-like budding in the host hemocoel requires a transition of cuticle-penetrating hyphae to unicellular hyphal bodies, namely, blastospores (32). This dimorphic transition is governed by the CDP activator genes *brlA* and *abaA* in *B. bassiana* (4). For insight into severely compromised virulence of the Δ*frq* mutants, hemolymph samples taken from the larvae surviving 4 days postinfection in either mode were examined under a microscope. As a result, hyphal bodies were abundant in the samples of the larvae infected by the control strains but hardly found in the samples of those infected by the Δ*frq1* and Δ*frq2* mutants (Fig. 1C), implicating a blockage of hyphal body development in both Δ*frq* mutants. This implication was clarified in the 3-day-old submerged cultures of a 10^6 conidia/ml suspension grown at an optimum of

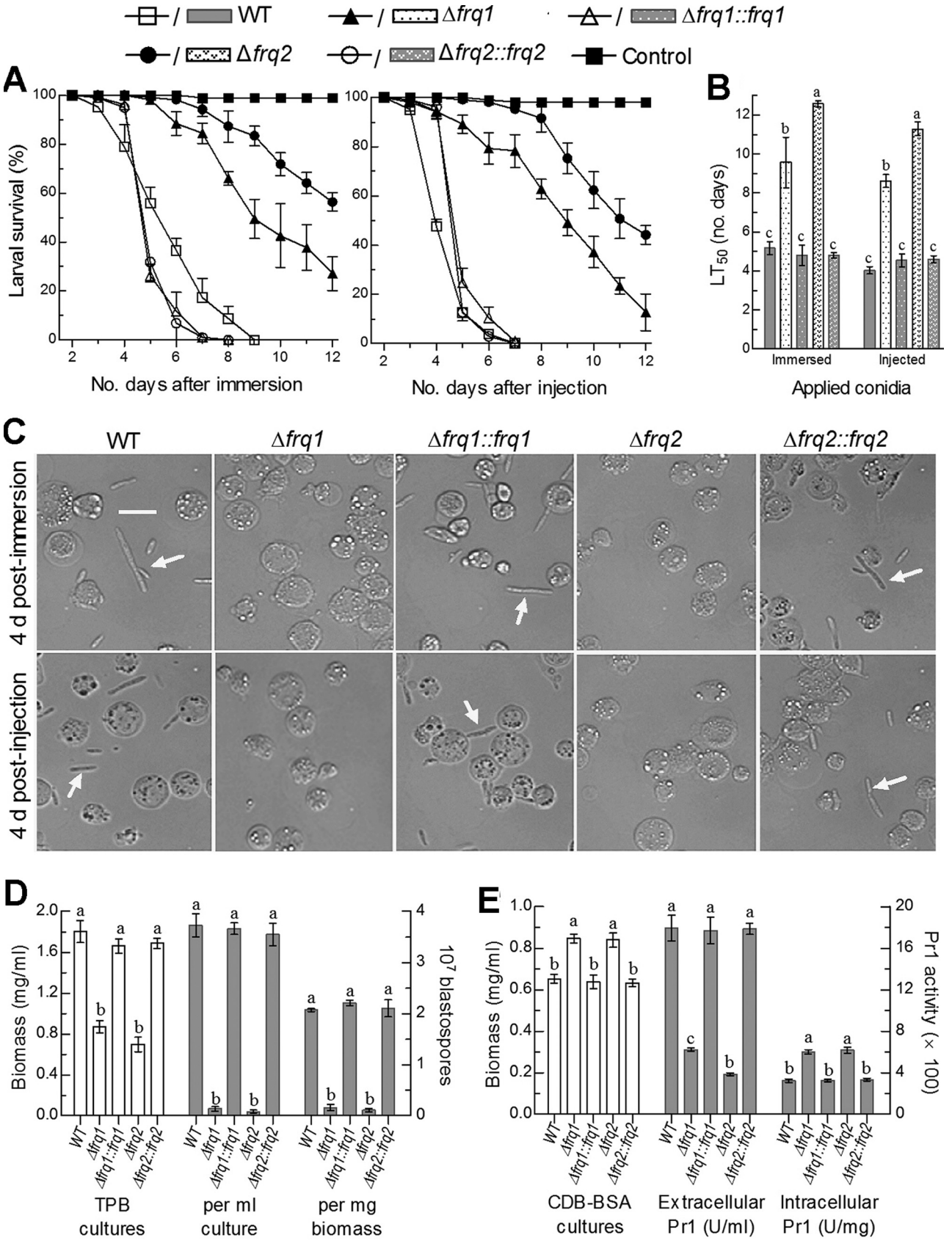

FIG 1 Requirements of *frq1* and *frq2* for the virulence and virulence-related cellular events of *B. bassiana*. (A) Survival trends of *G. mellonella* larvae after immersion in a 10^7 conidia/ml suspension for normal cuticle infection and injection with ~500 conidia per larva for cuticle-bypassing

(Continued on next page)

25°C in a trehalose-peptone broth (TPB) mimicking insect hemolymph. The resultant biomass levels in the Δ*frq1* and Δ*frq2* cultures decreased by 25% and 30%, respectively, in comparison to an estimate of 1.8 mg/ml from the WT cultures (Fig. 1D, left *y* axis). In contrast, blastospore concentrations were 96% and 98% lower in the TPB cultures of the two mutants than in those of the WT strain, resulting in a dimorphic transition rate per milligram biomass reduced by 92% in Δ*frq1* and 95% in Δ*frq2* (Fig. 1D, right *y* axis). These *in vitro* observations provide support for the blocked development of either Δ*frq1* or Δ*frq2* hyphal bodies *in vivo* but little clue to why there is significantly more attenuated virulence through either infection mode in the absence of *frq2* than in the absence of *frq2*.

Next, total activities of Pr1 proteases required for hyphal invasion into insect body through cuticular penetration were quantified from the 2-day-old cultures of a 10^6 conidia/ml suspension grown at 25°C in Czapek-Dox broth (CDB) containing the sole nitrogen source of 0.3% bovine serum albumin (BSA) as an enzyme inducer. The CDB cultures of both Δ*frq1* and Δ*frq2* mutants showed a similar biomass increase (~14%) in comparison to the WT biomass (Fig. 1E, left *y* axis). In contrast, total extracellular (secreted) Pr1 activities decreased by 65% and 78% in the supernatants of the Δ*frq1* and Δ*frq2* cultures, while total intracellular (synthesized) Pr1 activities increased by 85% and 91% in the protein extracts isolated from the same cultures of the two mutants, respectively, compared to the corresponding quantities from the WT strain (Fig. 1E, right *y* axis). These data indicate more blocked secretion of cuticle-degrading Pr1 proteases in the absence of *frq2* than in the absence of *frq1* and help to explain differential virulence reductions of the two mutants via normal cuticle infection.

Frq1 and Frq2 are essential for the infection cycle. The natural infection cycle of a fungal insect pathogen requires production of aerial conidia on the surfaces of mycosis-killed cadavers for infection to nearby hosts and dispersal in host habitats for new infection. Thus, conidiation capacity of insect cadavers is very important for both the prevalence of natural infection in insect populations and the pest control efficacy and persistence of a fungal insecticide applied in the field. Previous studies have revealed that, at or near the time of host death from mycosis, intrahemocoel hyphal bodies must turn back into normal hyphae to penetrate again through the insect cuticle for outgrowth and ultimate conidiation on cadaver surfaces (8, 18, 31, 33). To explore possible roles of Frq1 and Frq2 in the infection cycle of *B. bassiana*, conidial yields were quantified from the *G. mellonella* cadavers maintained for 9 and 12 days at 25°C in five light/dark (L:D) cycles covering full dark to full light. As shown in Fig. 2A, cadavers from larvae that were infected with the control strains were wrapped with a heavy layer of slightly yellowish outgrowths 9 days postdeath, contrasting to a thinner layer of more whitish outgrowths on those that were infected with the two Δ*frq* mutants. Revealed with scanning electronic microscopy (SEM), hyphal samples taken from the cadaver surfaces contained many more conidia of the WT strain than of either Δ*frq* mutant (Fig. 2B). As a consequence, conidial yields of three control strains on the cadavers in the L:D cycles of 0:24, 6:18, 12:12, 18:6, and 24:0 were averaged as 331×10^6, 386×10^6, 420×10^6, 521×10^6, and 563×10^6 conidia per cadaver 9 days postdeath (Fig. 2B, upper panel) and slightly increased to 358×10^6, 411×10^6, 459×10^6, 532×10^6, and 578×10^6 conidia per cadaver 12 days postdeath (Fig. 2B, lower panel), respectively. Compared to the control strains, the Δ*frq1* and Δ*frq2* mutants were compromised

FIG 1 Legend (Continued)
infection. (B) LT_{50} estimates (in days) for the resultant time-mortality trends of different fungal strains against the larvae. (C) Microscopic images (scale bar, 20 μm) of hyphal bodies (arrowed) and host hemocytes (spherical or subspherical cells) in the hemolymph samples taken from the larvae surviving 4 days after immersion and injection. (D) Biomass levels (white bars) of fungal strains in the 3-day-old cultures of a 10^6 conidia/ml TPB shaken at 25°C and blastospore yields (gray bars) per milliliter of TPB culture or per milligram of biomass (dimorphic transition rate). (E) Biomass levels (white bars) of fungal strains in the 2-day-old cultures of a 10^6 conidia/ml CDB-BSA shaken at 25°C and extra- and intracellular Pr1 activities (gray bars) quantified from the supernatants and protein extracts of the cultures. Different lowercase letters in each bar group denote significant differences (Tukey's honestly significant difference [HSD], $P < 0.05$). Each error bar indicates standard deviation of the mean from three independent replicates.

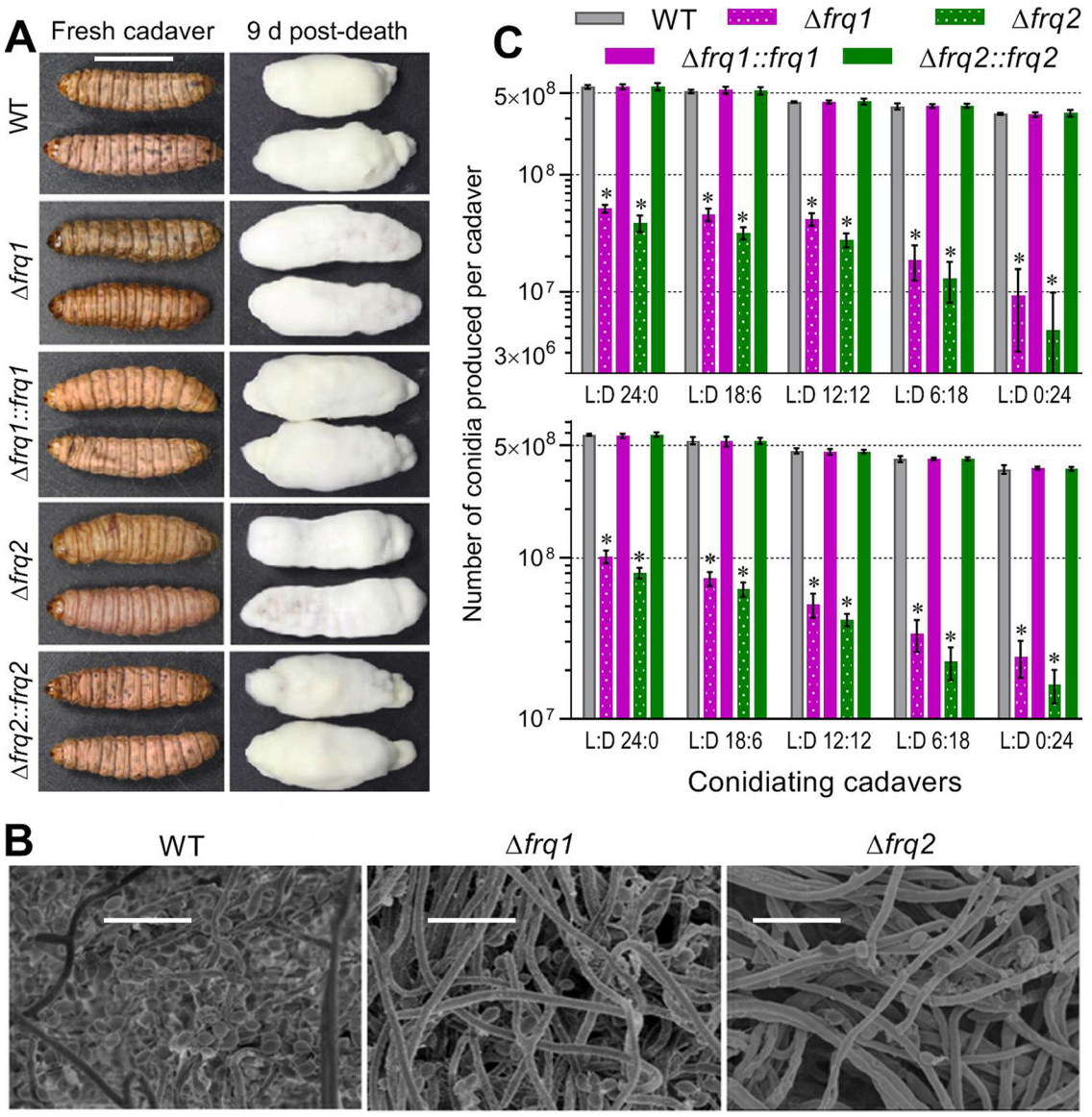

FIG 2 Essential roles of *frq1* and *frq2* for the infection cycle of *B. bassiana*. (A) Images (scale, 10 mm) of mycosis-killed *G. mellonella* cadavers and fungal outgrowths on the cadavers 9 days postdeath. (B) SEM images (scale bar, 10 μm) for conidiation status of the Δ*frq* and WT outgrowths on the surfaces of cadavers 9 days postdeath. (C) Conidial yields of fungal strains quantified from cadavers 9 and 12 days postdeath. The cadavers were maintained at 25°C in the indicated L:D cycles. The asterisked yields of the Δ*frq1* and Δ*frq2* mutants differ significantly from the unmarked yields of their control strains (Tukey's HSD, $P < 0.0001$). Each error bar indicates standard deviation of the mean from three replicates of three cadavers per sample.

severely in aerial conidiation on the cadavers. For the two mutants, conidial yields on cadaver surfaces 9 days postdeath decreased sharply by 97.2% and 98.6% at L:D 0:24 and by 90.9% and 93.1% at L:D 24:0, and the yield reductions 12 days postdeath diminished to 93.2% and 95.4% at L:D 0:24 and to 82.4% and 86.1% at L:D 24:0, respectively. In one-factor analysis of variance (ANOVA), the L:D cycles had significant impacts on the conidial yields of both the control strains ($F_{4,10} \geq 190.6$, $P < 0.0001$) and the Δ*frq* mutants ($F_{4,10} \geq 151.0$, $P < 0.0001$) on insect cadavers, implicating a substantial decrease of conidiation level *in vivo* with shortening daylight length. These data demonstrate essential roles of both Frq1 and Frq2 in conidial production of insect cadavers for the infection cycle of *B. bassiana* in host habitats with seasonal or geographic photoperiod change.

Frq1 and Frq2 function in calcofluor-specific signaling through the MAPK Slt2 cascade. For further insight into the fungal virulence differentially compromised in the two Δ*frq* mutants, colonies of each strain initiated with 1-μl aliquots of a 10^6 conidia/ml suspension were examined for a capability of radial growth under normal and stressful conidiations since hyphal invasion into insect body and subsequent proliferation in the host hemocoel are challenged by oxidative stress of reactive oxygen species generated from host immunity defenses and high osmolarity in trehalose-concentrated host hemolymph (29, 34). All of the Δ*frq* mutants and the control strains showed little variability in radial growth on rich SDAY (Sabouraud dextrose agar plus yeast extract), 1/4 SDAY (1/4 strength of each SDAY nutrient), or minimal CDA (Czapek-Dox agar) after an 8-day incubation at the optimal regime of 25°C and L:D 12:12 (Fig. 3A), although conidial germination at 25°C was slower in the absence of *frq1* or *frq2* (Fig. 3B). Also, all of the tested strains showed similar responses to oxidative stress of H_2O_2 or menadione, hyperosmotic stress of NaCl or sorbitol, and cell wall-perturbing stress of Congo red (Fig. 3C), respectively, during 10-day growth at 25°C on the CDA plates supplemented with the stress agents ($P > 0.05$ for a variability of measured diameters [data not shown] in one-factor [strain] ANOVA). Exceptionally, the mean diameter of colonies cocultivated with calcofluor white (6 μg/ml), another cell wall antagonist, decreased by 84% in the Δ*frq1* mutant but increased by 46% in the Δ*frq2* mutant versus that of the WT strain. The hypersensitivity of the Δ*frq1* mutant to cell wall perturbation was evidenced with increased cell wall fragility of its conidia, which were readily impaired in a routine pretreatment for SEM (Fig. 3D). Interestingly, the Δ*frq2* conidia were deformed after the pretreatment in comparison to the pretreated WT conidia with a well-defined intact coat of hydrophobin-borne rodlet bundles (35), hinting at a conidial cell wall plasticity compromised in the absence of *frq2*.

The hypersensitivity of the Δ*frq1*mutant and the high resistance of the Δ*frq2* mutant to calcofluor white suggest involvements of Frq1 and Frq2 in the signal transduction through the MAPK Slt2 cascade that serves as the CWI signaling pathway in *B. bassiana* (28). This speculation was examined through Western blotting of expressed Slt2 and phosphorylated Slt2 in the protein extracts of hyphal cultures triggered for 30 min with or without calcofluor white (6 μg/ml). For all of the Δ*frq* and control strains, the blots of expressed Slt2 probed with an anti-Mpk1 (yN-19) antibody and those of expressed β-actin (internal standard) probed with an anti-actin antibody were similar in size and intensity irrespective of being triggered with or without the chemical (Fig. 3E, two lower rows in each panel). After 30-min treatment with calcofluor white, intriguingly, the signal of phosphorylated Slt2 (P-Slt2) probed with an anti-phospho-p44/p42 MAPK antibody was markedly attenuated in the Δ*frq1* mutant but greatly intensified in the Δ*frq2* mutant in comparison to similar signals of the control strains (Fig. 3E, upper row in each panel). However, no P-Slt2 signal appeared in the extracts from the cultures of all tested strains not triggered with the chemical. For the Δ*frq1* and Δ*frq2* mutants, the opposite P-Slt2 signal changes coincided well with their opposite responses to the cell wall antagonist, implicating a blockage of Slt2 phosphorylation in the absence of *frq1* and of Slt2 dephosphorylation in the absence of *frq2*. These results unveil novel roles of Frq1 and Frq2 in calcofluor-specific signal transduction through the MAPK Slt2 cascade in *B. bassiana*.

DISCUSSION

In *B. bassiana*, both Frq1 and Frq2 were proven to be essential for conidial production of mycosis-killed insect cadavers crucial for the fungal infection cycle in host habitats with seasonal or geographic photoperiod changes. The severe conidiation defects of our Δ*frq1* and Δ*frq2* mutants on insect cadavers were mitigated with an increase of daylight length. Such defects are consistent with their *in vitro* conidiation defects, which were compromised with shortening daylight length and attributed to differentially reduced transcript levels of three CDP genes in different L:D cycles (15). The repressed expression levels of the CDP genes indispensable for the fungal conidiation

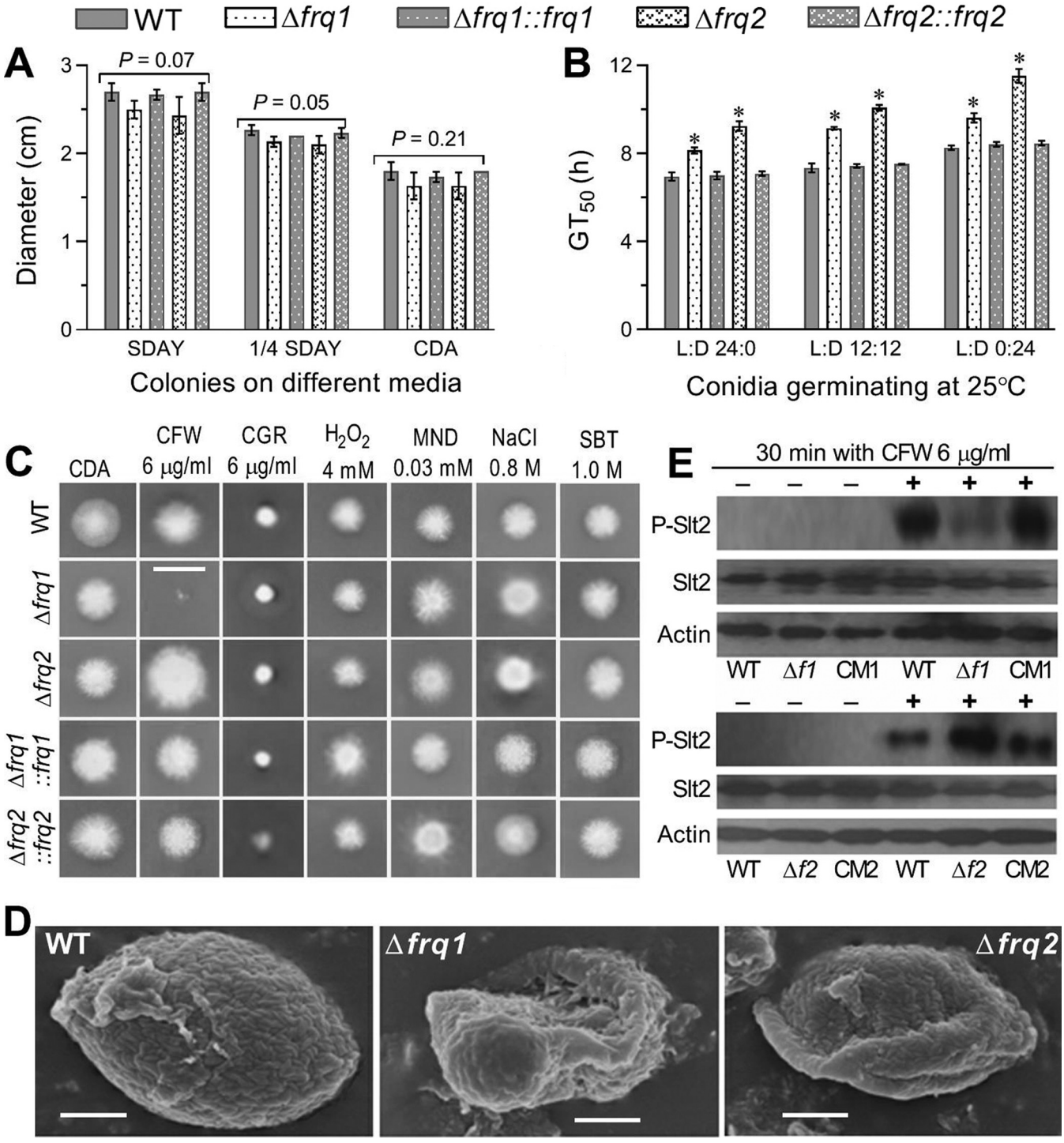

FIG 3 Impacts of *frq1* or *frq2* deletion on the growth of *B. bassiana* under normal and stressful conditions. (A) Diameters of fungal colonies after an 8-day incubation on SDAY, 1/4 SDAY, and CDB at the optimal regime of 25°C and L:D 12:12. (B) Time for 50% conidial germination (GT_{50}) at 25°C in the three indicated L:D cycles. (C) Images (scale bar, 2 cm) of fungal colonies grown at 25°C for 10 days on CDA containing CFW (calcofluor white), CGR (Congo red), H_2O_2, MND (menadione), NaCl, and SBT (sorbitol) at the indicated concentrations, respectively. Each colony was initiated by spotting 1 μl of a 10^6 conidia/ml suspension. (D) SEM images (scale bar, 0.5 μm) for ultrastructural views of conidial surfaces. Note the increased fragility and reduced plasticity of conidial coat for the Δ*frq1* and Δ*frq2* mutants, respectively, in comparison to an integrity of conidial coat for the WT strain. (E) Western blots of phosphorylated Slt2 (P-Slt2), expressed Slt2, and expressed β-actin (reference) in the hyphal cells triggered for 30 min with (+) or without (−) CFW (6 μg/ml). Each lane was uploaded with 60-μg protein extract. Δ*f1* and CM1, Δ*frq1* and Δ*frq1*::*frq1*. Δ*f2* and CM2, Δ*frq2* and Δ*frq2*::*frq2*. The means represented by asterisked bars in each bar group (B) differ significantly from those of the unmarked bars (Tukey's HSD, $P < 0.01$). Each error bar (A, B) indicates standard deviation of the mean from three independent replicates.

(4) also coincide well with the severe conidiation defects of the two Δ*frq* mutants on the insect cadavers in this study. Previously, opposite rhythms of Frq1 and Frq2 in nucleus were shown to present a total FRQ level that is relatively stable and high enough to persistently activate the CDP genes in a circadian day and hence to support the nonrhythmic conidiation for maximization of conidial yield independent of photoperiods, the change of which from L:D 0:24 to L:D 24:0 resulted in only a 2-day difference for the control strains to reach similar maxima of conidial yields (15). While the previous study revealed essential roles of both Frq1 and Frq2 in orchestrating the fungal nonrhythmic conidiation *in vitro*, the present study reinforces an indispensability of either Frq1 or Frq2 for the fungal infection cycle in host habitats. However, we failed to create double deletion mutants of both *frq1* and *frq2* in many attempts, implicating a requirement of one *frq* gene for the fungal survival in the absence of the other. Taken together with the results in the previous and present studies, coexistence of Frq1 and Frq2 in *B. bassiana* endows a relatively high stability of total nuclear FRQ level that persistently activates the CDP genes in a circadian day to not only sustain the fungal infection cycle in host habitats but also favor large-scale rapid production of conidia as active ingredients of the fungal formulations against arthropod pests.

The insect pathogenicity severely compromised in our Δ*frq1* and Δ*frq2* mutants indicates an essentiality of either Frq1 or Frq2 for the fungal virulence, which is dependent on a capability of hyphal invasion into insect body and a speed of subsequent intrahemocoel propagation by yeast-like budding. This finding is consistent with the regulatory role of a circadian oscillator in the virulence of *Botrytis cinerea* when infecting *Arabidopsis thaliana* (36). In *B. bassiana*, a loss of almost all virulence through normal cuticle infection is often associated with severe growth defects on scant media close to oligotrophic insect integument, such as the cases caused by the disruption of *fus3*, *ste7*, or *ste11* in the MAPK Fus3 cascade (13, 14) and a blockage of carbon/nitrogen metabolisms in the absence of *gcn5* (9), *ubi4* (17), *ssr4* (18), or *rei1* (33). In this study, moderate Δ*frq1* and Δ*frq2* defects in conidial germination exerted insignificant impact on their radial growths on rich and scant media. Biomass levels of aerial hyphae in the SDAY cultures used for estimation of conidial yields also showed no difference between the two mutants and the control strains (15). Apparently, no growth defect is accountable for the reduced virulence of either Δ*frq* mutant. Revealed in the analyses of postinfection cellular events crucial for virulence, blocked dimorphic transition in insect hemolymph or submerged conditions mimicking insect hemolymph is a main cause of virulence attenuation in the absence of *frq1* or *frq2*. This implication is in the previous evidence with transcriptional repression of the key CDP genes *brlA* and *abaA* (15) that serve as master regulators of dimorphic transition in *B. bassiana* (4). However, the blockage of dimorphic transition alone is insufficient to distinguish marked virulence differences between the two Δ*frq* mutants in two infection modes.

The greater importance of Frq2 than of Frq1 for the fungal virulence is presented by a delay of ~3 days in median lethal action of the Δ*frq2* versus that of the Δ*frq1* mutant against the model insect in either infection mode. A relatively small (13%) difference in extracellular Pr1 activity required for cuticular penetration in the infection course of *B. bassiana* (31) is unlikely to be causative of the big virulence difference between the two mutants via intrahemocoel injection, although reduced secretions of Pr1 proteases are obviously responsible for large parts of their virulence losses (65% in Δ*frq1* and 78% in Δ*frq2*) via the normal infection. This hints at involvement of Frq1 and Frq2 in some other postinfection cellular events associated with virulence, such as fungal responses to possible stress cues encountered after entry into the host hemocoel (29, 34). As a consequence of stress assay *in vitro*, both deletion mutants showed null responses to two oxidants, two osmotic agents, and the cell wall stressor Congo red. Surprisingly, radial growth in the presence of calcofluor white was sharply suppressed in the Δ*frq1* mutant but largely facilitated in the Δ*frq2* mutant. Calcofluor white is a cell wall antagonist that has been used for genome-wide screen of sensitive and resistant yeast genes associated with MAPK signaling pathway, *N*-glycan biosynthesis,

endocytosis, vacuole acidification, autophagy, and sulfur relay system (37). The chemical is also a chitin-specific stain used for rapid quantification of chitin in homogenized insect samples (38) and histopathological diagnosis of subcutaneous mycosis (39). The hypersensitivity of the Δ*frq1* mutant and the high resistance of the Δ*frq2* mutant to the cell wall antagonist indicate opposite roles of Frq1 and Frq2 in calcofluor-specific response of *B. bassiana* and also implicate their involvement in the CWI signaling pathway, which orchestrates changes in the cell wall through the cell cycle in yeast (reviewed in reference 40) and filamentous fungi (reviewed in reference 27). This implication was confirmed by hypo- and hyperphosphorylation of Slt2 in the Δ*frq1* and Δ*frq2* cells triggered with calcofluor white. The MAPK Slt2/Mpk1 regulates many nuclear targets, including the SBF complex that is formed by DNA-binding components, and serves as a transcriptional activator of cell cycle-dependent genes and the MADS-box transcription factor, which regulates many genes involved in cell wall biogenesis and function (27). While the hypersensitivity of the Δ*frq1* mutant to the cell wall antagonist coincides with the increased cell wall fragility of its conidia observed via SEM, the reduced cell wall plasticity of the Δ*frq2* conidia seemed to conflict with its high resistance to the cell wall stress, implying that some other cellular events affecting the cell wall plasticity are likely associated with the target genes regulated by Slt2. Previously, deletion of *slt2* in *B. bassiana* resulted in a delay of median lethal action (against *G. mellonella*) by 0.85-fold in the normal infection and by 0.6-fold via injection and also abolished phosphorylation of the MAPK Hog1 (28), suggesting an interplay between the fungal Slt2 and Hog1 signaling cascades. Interestingly, the blocked Slt2 phosphorylation in the Δ*frq1* response to calcofluor white corresponds to the same level of virulence loss as did the *slt2* deletion via the normal infection but to greater virulence loss via the injection. Moreover, the blocked Slt2 dephosphorylation in the Δ*frq2* response to the same chemical cue corresponds to far more virulence loss in both infection modes. These findings uncover opposite, but essential, roles for Frq1 and Frq2 in calcofluor-specific signal transduction through the Slt2 cascade in *B. bassiana* and an importance of such signaling roles for the fungal virulence to insect. We speculate that a blockage of Slt2 phosphorylation or dephosphorylation could have caused malfunctions of its multiple nuclear targets, which may regulate genome-wide gene expression likely associated with the big virulence difference between the Δ*frq1* and Δ*frq2* mutants.

Altogether, our findings unveil essential roles for two FRQ proteins in sustaining both the virulence and the infection cycle of *B. bassiana* and provide novel insight into their opposite roles in the calcofluor-specific signal transduction through the fungal CWI signaling pathway. However, it remains unclear what possible checkpoint (or checkpoints) links Frq1 and Frq2 to the fungal Slt2 cascade in response to the specific cue, warranting further studies.

MATERIALS AND METHODS

Fungal strains and cultures. The Δ*frq1* and Δ*frq2* deletion mutants of the WT strain (*B. bassiana* ARSEF 2860) and the Δ*frq1*::*frq1* and Δ*frq2*::*frq2* complementation strains were created and identified through PCR and Southern blotting in our previous study (15). All mutant and control strains were incubated on the standard medium SDAY (4% glucose, 1% peptone, 1% yeast extract, and 1.5% agar) for full conidiation at the optimal regime of 25°C and L:D 12:12. Conidia from the cultures were used in the following experiments of three independent replicates.

Experiments for phenotypic changes. For each strain, 80-μl aliquots of a 10^7 conidia/ml suspension were evenly spread on thin agar plates containing 2% sucrose and 0.5% peptone and incubated for germination at 25°C. During the incubation, germinated and nongerminated conidia on each plate were counted every 2 h from three fields of microscopic view (100× magnification) until full germination. Time (h) for 50% conidial germination (GT_{50}) at the optimal temperature was estimated as an index of conidial viability by modeling analysis of the resultant germination trends over the time of incubation.

Each of the strains was grown on the plates of SDAY, 1/4 SDAY, and CDA (3% sucrose, 0.3% $NaNO_3$, 0.1% K_2HPO_4, 0.05% KCl, 0.05% $MgSO_4$, 0.001% $FeSO_4$, and 1.5% agar) by spotting 1-μl aliquots of a 10^6 conidia/ml suspension. After an 8-day incubation at the optimal regime, the mean diameter of each colony was estimated as an index of radial growth with two measurements taken perpendicular to each other across the colony center.

The spotting method was also used to initiate radial growth of each strain on CDA plates supplemented

with a sensitive concentration of each of the stress agents used in our previous study (41): (i) H_2O_2 (4 mM) or menadione (0.03 mM) for response to oxidative stress; (ii) NaCl (0.8 M) or sorbitol (1 M) for response to hyperosmotic stress; and (iii) Congo red (6 μg/ml) or calcofluor white (6 μg/ml) for response to cell wall-perturbing stress. After a 10-day incubation with the stress agents at the optimal regime, the diameter of each colony was estimated as aforementioned, and typical colonies of all strains were photographed.

Assays for fungal virulence and virulence-related cellular events. Two types of standardized bioassays were carried out to assess the virulence of each strain against the fifth-instar larvae of *G. mellonella*. First, three groups of larvae (35 to 40 per group) per strain were immersed for 10 s in 40-ml aliquots of a 10^7 conidia/ml suspension to initiate normal cuticle infection. Second, 5 μl of a 10^5 conidia/ml suspension was injected into the hemocoel of each larva in each group for cuticle-bypassing infection. Three groups of larvae immersed in 40-ml aliquots of, or individually injected with 5-μl aliquots of, 0.02% Tween 80 were used as controls of each bioassay. All treated groups were maintained at 25°C and monitored daily for 12 days of survival/mortality records. The resultant time-mortality trend in each group was subjected to probit analysis, generating an LT_{50} (in days) as a virulence index.

Examination of cellular processes crucial for virulence and infection cycle. During the bioassays, hemolymph samples taken from the larvae surviving 4 days after immersion or injection were observed under a microscope to reveal the presence/absence and abundance of hyphal bodies, namely, possible differences in dimorphic transition *in vivo* between the Δ*frq* mutants and the control strains. Next, 50-ml aliquots of a 10^6 conidia/ml suspension in TPB, namely, CDB (i.e., agar-free CDA) amended with 3% trehalose as sole carbon source and 0.5% peptone as sole nitrogen source to mimic insect hemolymph, were incubated for 3 days on a shaking bed (150 rpm) at 25°C. The concentration of blastospores in each submerged culture was assessed with a hemocytometer. All cells were collected from the culture through filtration and dried overnight at 50°C, followed by quantification of biomass level (mg/ml). The two quantities were used to compute the number of blastospores produced per milligram of biomass as an index of dimorphic transition *in vitro*.

Total activities of Pr1 proteases collectively required for cuticular penetration during hyphal invasion of *B. bassiana* into insect body (31) were assayed at extracellular (secreted) and intracellular (synthesized) levels from submerged CDB-BSA cultures of each strain as described previously (8). Briefly, 100-ml aliquots of a 10^6 conidia/ml suspension in CDB-BSA were incubated on the shaking bed for 2 days at 25°C, followed by centrifugation at 4°C. Half of hyphal biomass in each culture was assessed as aforementioned, and another half was ground in liquid nitrogen for protein extraction immediately after centrifugation. Total activity of extracellular Pr1 proteases in each supernatant (crude extract) or of intracellular Pr1 proteases in each protein extract was assessed by reading optical density at 410 nm (OD_{410}). One unit of Pr1 activity was defined as an enzyme amount required for an OD_{410} increase by 0.01 after a 1-h reaction of each extract versus a control. Extra- or intracellular Pr1 activity was expressed as the number of units per milliliter of supernatant or per milligram of protein extract.

Cadavers from insects that died from the normal infection of each fungal strain were maintained for 12 days of fungal outgrowths at 25°C in the respective L:D cycles of 0:24, 6:18, 12:12, 18:6, and 24:0. Fresh cadavers and those 9 days postdeath were photographed. A sample of every three cadavers 9 or 12 days postdeath were placed in 10-ml aliquots of 0.02% Tween 80, followed by supersonic vibration for the release of conidia into the surfactant solution from each sample. The conidial concentration of the resultant suspension was assessed with a hemocytometer and converted to the number of conidia produced per cadaver. Three samples were assessed per fungal strain on each sampling occasion. The conidial yield on cadaver surfaces was used as an index of fungal infection cycle in host habitats. In addition, conidiation status of hyphal samples and conidia taken from cadaver surfaces 9 days postdeath were examined through SEM after a routine pretreatment.

Western blot for expressed Slt2 and phosphorylated Slt2. The 50-ml aliquots of a 10^6 conidia/ml suspension in SDBY (i.e., agar-free SDAY) were incubated on the shaking bed for 3 days at 25°C. Hyphae and blastospores collected from the cultures of each strain were repeatedly washed with sterile water, resuspended in equal volumes of CDB alone (control) or supplemented with calcofluor white 6 μg/ml (treatment), and then incubated for 30 min at 25°C. Our previous protocols (41) were used to isolate protein extracts from the stressed cultures of each Δ*frq* mutant and control strains and to probe expressed and phosphorylated signals of Slt2 in Western blot experiments. Briefly, the homogenized product ground in liquid nitrogen was suspended in 20 mM phosphate-buffered saline (PBS; pH 7.0) supplemented with protease inhibitor cocktail (Amresco, Solon, OH, USA) and phosphatase inhibitors (Thermo Fisher Scientific, Rockford, IL, USA). The mixture was vibrated for 30 s three times at an interval of 60 s on ice, followed by 15-min centrifugation at 15,000 $\times$ *g* at 4°C. Protein extract samples of 60 μg (standardized by dilution) were loaded onto 12% SDS-PAGE and transferred to polyvinylidene difluoride (PVDF) membranes (Millipore, Germany). The expressed and phosphorylated signals of Slt2 on the sample-loaded PVDF membranes were probed with the respective 1,000-fold dilutions of an anti-Mpk1 (yN-19) antibody (Santa Cruz Biotechnology, Santa Cruz, CA, USA) and an anti-phospho-p44/p42 MAPK antibody (Cell Signaling Technology, Danvers, MA, USA). The signal of expressed β-actin protein probed with an anti-actin antibody (Cell Signaling Technology) was used as a reference. The bound antibodies were reacted with 7,500-fold dilution of horseradish peroxidase (HRP) conjugated anti-rabbit antibodies (Cell Signaling Technology) and visualized in a chemiluminescence detection system (ECL Amersham Biosciences).

ACKNOWLEDGMENTS

Funding of this work was provided by the National Natural Science Foundation of China (grants 31801795 and 31772218) and the Ministry of Science and Technology of the People's Republic of China (grant 2017YFD0201202). We declare no conflict of interest.

REFERENCES

1. Otamendi A, Espeso EA, Etxebeste O. 2019. Identification and characterization of *Aspergillus nidulans* mutants impaired in asexual development under phosphate stress. Cells 8:1520. https://doi.org/10.3390/cells8121520.
2. Etxebeste O, Garzia A, Espeso EA, Ugalde U. 2010. *Aspergillus nidulans* asexual development: making the most of cellular modules. Trends Microbiol 18:569–576. https://doi.org/10.1016/j.tim.2010.09.007.
3. Park HS, Yu JH. 2012. Genetic control of asexual sporulation in filamentous fungi. Curr Opin Microbiol 15:669–677. https://doi.org/10.1016/j.mib.2012.09.006.
4. Zhang AX, Mouhoumed AZ, Tong SM, Ying SH, Feng MG. 2019. BrlA and AbaA govern virulence-required dimorphic switch, conidiation and pathogenicity in a fungal insect pathogen. mSystems 4:e00140-19. https://doi.org/10.1128/mSystems.00140-19.
5. Li F, Shi HQ, Ying SH, Feng MG. 2015. WetA and VosA are distinct regulators of conidiation capacity, conidial quality, and biological control potential of a fungal insect pathogen. Appl Microbiol Biotechnol 99:10069–10081. https://doi.org/10.1007/s00253-015-6823-7.
6. Zhu J, Ying SH, Feng MG. 2016. The Na^+/H^+ antiporter Nhx1 controls vacuolar fusion indispensible for life cycle *in vitro* and *in vivo* in a fungal insect pathogen. Environ Microbiol 18:3884–3895. https://doi.org/10.1111/1462-2920.13359.
7. Chu ZJ, Sun HH, Zhu XG, Ying SH, Feng MG. 2017. Discovery of a new intravacuolar protein required for the autophagy, development and virulence of *Beauveria bassiana*. Environ Microbiol 19:2806–2818. https://doi.org/10.1111/1462-2920.13803.
8. Tong SM, Zhang AX, Guo CT, Ying SH, Feng MG. 2018. Daylight length-dependent translocation of VIVID photoreceptor in cells and its essential role in conidiation and virulence of *Beauveria bassiana*. Environ Microbiol 20:169–185. https://doi.org/10.1111/1462-2920.13951.
9. Cai Q, Wang JJ, Fu B, Ying SH, Feng MG. 2018. Gcn5-dependent histone H3 acetylation and gene activity is required for the asexual development and virulence of *Beauveria bassiana*. Environ Microbiol 20:1484–1497. https://doi.org/10.1111/1462-2920.14066.
10. Wang JJ, Cai Q, Qiu L, Ying SH, Feng MG. 2018. The histone acetyltransferase Mst2 sustains the biological control potential of a fungal insect pathogen through transcriptional regulation. Appl Microbiol Biotechnol 102:1343–1355. https://doi.org/10.1007/s00253-017-8703-9.
11. Cai Q, Wang ZK, Shao W, Ying SH, Feng MG. 2018. Essential role of Rpd3-dependent lysine modification in the growth, development and virulence of *Beauveria bassiana*. Environ Microbiol 20:1590–1606. https://doi.org/10.1111/1462-2920.14100.
12. Cai Q, Tong SM, Shao W, Ying SH, Feng MG. 2018. Pleiotropic effects of the histone deacetylase Hos2 linked to H4-K16 deacetylation, H3-K56 acetylation and H2A-S129 phosphorylation in *Beauveria bassiana*. Cell Microbiol 20:e12839. https://doi.org/10.1111/cmi.12839.
13. Wang ZK, Cai Q, Tong SM, Ying SH, Feng MG. 2018. C-terminal Ser/Thr residues are vital for the regulatory role of Ste7 in the asexual cycle and virulence of *Beauveria bassiana*. Appl Microbiol Biotechnol 102:6973–6986. https://doi.org/10.1007/s00253-018-9148-5.
14. Liu J, Wang ZK, Sun HH, Ying SH, Feng MG. 2017. Characterization of the Hog1 MAPK pathway in the entomopathogenic fungus *Beauveria bassiana*. Environ Microbiol 19:1808–1821. https://doi.org/10.1111/1462-2920.13671.
15. Tong SM, Wang DY, Cai Q, Ying SH, Feng MG. 2020. Opposite nuclear dynamics of two FRH-dominated frequency proteins orchestrate non-rhythmic conidiation of *Beauveria bassiana*. Cells 9:626. https://doi.org/10.3390/cells9030626.
16. Wang DY, Mou YN, Tong SM, Ying SH, Feng MG. 2020. Photoprotective role of photolyase-interacting RAD23 and its pleiotropic effect on the insect-pathogenic fungus *Beauveria bassiana*. Appl Environ Microbiol 86:e00287-20. https://doi.org/10.1128/AEM.00287-20.
17. Wang DY, Ren K, Tong SM, Ying SH, Feng MG. 2020. Pleiotropic effects of Ubi4, a polyubiquitin precursor required for ubiquitin accumulation, conidiation and pathogenicity of a fungal insect pathogen. Environ Microbiol 22:2564–2580. https://doi.org/10.1111/1462-2920.14940.
18. Shao W, Cai Q, Tong SM, Ying SH, Feng MG. 2020. Nuclear Ssr4 is required for the *in vitro* and *in vivo* asexual cycles and global gene activity of *Beauveria bassiana*. mSystems 5:e00677-19. https://doi.org/10.1128/mSystems.00677-19.
19. Tong SM, Feng MG. 2020. Phenotypic and molecular insights into heat tolerance of formulated cells as active ingredients of fungal insecticides. Appl Microbiol Biotechnol 104:5711–5724. https://doi.org/10.1007/s00253-020-10659-z.
20. Colot HV, Loros JJ, Dunlap JC. 2005. Temperature-modulated alternative splicing and promoter use in the Circadian clock gene frequency. Mol Biol Cell 16:5563–5571. https://doi.org/10.1091/mbc.e05-08-0756.
21. Diernfellner A, Colot HV, Dintsis O, Loros JJ, Dunlap JC, Brunner M. 2007. Long and short isoforms of *Neurospora* clock protein FRQ support temperature-compensated circadian rhythms. FEBS Lett 581:5759–5764. https://doi.org/10.1016/j.febslet.2007.11.043.
22. Diernfellner AC, Querfurth C, Salazar C, Hofer T, Brunner M. 2009. Phosphorylation modulates rapid nucleocytoplasmic shuttling and cytoplasmic accumulation of *Neurospora* clock protein FRQ on a circadian time scale. Genes Dev 23:2192–2200. https://doi.org/10.1101/gad.538209.
23. Baker CL, Loros JJ, Dunlap JC. 2012. The circadian clock of *Neurospora crassa*. FEMS Microbiol Rev 36:95–110. https://doi.org/10.1111/j.1574-6976.2011.00288.x.
24. Hurley JM, Loros JJ, Dunlap JC. 2016. Circadian oscillators: around the transcription-translation feedback loop and on to output. Trends Biochem Sci 41:834–846. https://doi.org/10.1016/j.tibs.2016.07.009.
25. Salichos L, Rokas A. 2010. The diversity and evolution of circadian clock proteins in fungi. Mycologia 102:269–278. https://doi.org/10.3852/09-073.
26. Wang CS, Feng MG. 2014. Advances in fundamental and applied studies in China of fungal biocontrol agents for use against arthropod pests. Biol Control 68:129–135. https://doi.org/10.1016/j.biocontrol.2013.06.017.
27. Rispail N, Soanes DM, Ant C, Czajkowski R, Grünler A, Huguet R, Perez-Nadales E, Poli A, Sartorel E, Valiante V, Yang M, Beffa R, Brakhage AA, Gow NAR, Kahmann R, Lebrun MH, Lenasi H, Perez-Martin J, Talbot NJ, Wendland J, Di Pietro A. 2009. Comparative genomics of MAP kinase and calcium-calcineurin signaling components in plant and human pathogenic fungi. Fungal Genet Biol 46:287–298. https://doi.org/10.1016/j.fgb.2009.01.002.
28. Chen Y, Zhu J, Ying SH, Feng MG. 2014. Three mitogen-activated protein kinases required for cell wall integrity contribute greatly to biocontrol potential of a fungal entomopathogen. PloS One 9:e87948. https://doi.org/10.1371/journal.pone.0087948.
29. Tong SM, Feng MG. 2019. Insights into regulatory roles of MAPK-cascaded pathways in multiple stress responses and life cycles of insect and nematode mycopathogens. Appl Microbiol Biotechnol 103:577–587. https://doi.org/10.1007/s00253-018-9516-1.
30. Ortiz-Urquiza A, Keyhani NO. 2013. Action on the surface: entomopathogenic fungi versus the insect cuticle. Insects 4:357–374. https://doi.org/10.3390/insects4030357.
31. Gao BJ, Mou YN, Tong SM, Ying SH, Feng MG. 2020. Subtilisin-like Pr1 proteases marking evolution of pathogenicity in a wide-spectrum insect-pathogenic fungus. Virulence 11:365–380. https://doi.org/10.1080/21505594.2020.1749487.
32. Lewis MW, Robalino IV, Keyhani NO. 2009. Uptake of the fluorescent probe FM4-64 by hyphae and haemolymph-derived *in vivo* hyphal bodies of the entomopathogenic fungus *Beauveria bassiana*. Microbiology (Reading) 155:3110–3120. https://doi.org/10.1099/mic.0.029165-0.
33. Shao W, Cai Q, Tong SM, Ying SH, Feng MG. 2019. Rei1-like protein regulates nutritional metabolism and transport required for the asexual cycle *in vitro* and *in vivo* of a fungal insect pathogen. Environ Microbiol 21:2772–2786. https://doi.org/10.1111/1462-2920.14616.

34. Zhang LB, Feng MG. 2018. Antioxidant enzymes and their contributions to biological control potential of fungal insect pathogens. Appl Microbiol Biotechnol 102:4995–5004. https://doi.org/10.1007/s00253-018-9033-2.
35. Zhang SZ, Xia YX, Kim B, Keyhani NO. 2011. Two hydrophobins are involved in fungal spore coat rodlet layer assembly and each play distinct roles in surface interactions, development and pathogenesis in the entomopathogenic fungus, *Beauveria bassiana*. Mol Microbiol 80:811–826. https://doi.org/10.1111/j.1365-2958.2011.07613.x.
36. Hevia MA, Canessa P, Müller-Esparza H, Larrondo LF. 2015. A circadian oscillator in the fungus *Botrytis cinerea* regulates virulence when infecting *Arabidopsis thaliana*. Proc Natl Acad Sci U S A 112:8744–8749. https://doi.org/10.1073/pnas.1508432112.
37. Zhao FG, Li JW, Lin KR, Chen H, Lin Y, Zheng SP, Liang SL, Han SY. 2019. Genome-wide screening of *Saccharomyces cerevisiae* deletion mutants reveals cellular processes required for tolerance to the cell wall antagonist calcofluor white. Biochem Biophys Res Commun 518:1–6. https://doi.org/10.1016/j.bbrc.2019.07.057.
38. Henriques BS, Garcia ES, Azambuja P, Genta FA. 2020. Determination of chitin content in insects: an alternate method based on calcofluor staining. Front Physiol 11:117. https://doi.org/10.3389/fphys.2020.00117.
39. Liu XY, Liang GZ, Guo J, Duan XS, Li BQ, Xu Y, Wang SX, Lu J. 2019. Application of modified calcofluor white fluorescence staining in histopathological diagnosis of subcutaneous mycosis. Chin J Dermatol 52:319–322. https://doi.org/10.3760/cma.j.issn.0412-4030.2019.05.005.
40. Levin DE. 2005. Cell wall integrity signaling in *Saccharomyces cerevisiae*. Microbiol Mol Biol Rev 69:262–291. https://doi.org/10.1128/MMBR.69.2.262-291.2005.
41. Tong SM, Wang DY, Gao BJ, Ying SH, Feng MG. 2019. The DUF1996 and WSC domain-containing protein Wsc1l acts as a novel sensor of multiple stress cues in *Beauveria bassiana*. Cell Microbiol 21:e13100. https://doi.org/10.1111/cmi.13100.